Title

The Fragile X Proteins Differentially Regulate Translation of Reporter mRNAs with G-quadruplex Structures

Journal

Journal of Molecular Biology, 434(2)

ISSN

0022-2836

Authors

Edwards, Madison
Joseph, Simpson

Publication Date

2022

DOI

10.1016/j.jmb.2021.167396

Peer reviewed

HHS Public Access

Author manuscript

J Mol Biol. Author manuscript; available in PMC 2023 January 30.

Published in final edited form as:

J Mol Biol. 2022 January 30; 434(2): 167396. doi:10.1016/j.jmb.2021.167396.

The Fragile X Proteins Differentially Regulate Translation of Reporter mRNAs with G-quadruplex Structures

Madison Edwards, **Simpson Joseph***

Department of Chemistry and Biochemistry, University of California at San Diego, 9500 Gilman Drive, La Jolla, CA 92093-0314 USA

Abstract

Fragile X Syndrome, as well as some manifestations of autism spectrum disorder, results from improper RNA regulation due to a deficiency of fragile X mental retardation protein (FMRP). FMRP and its autosomal paralogs, fragile X related proteins 1 & 2 (FXR1P/2P), have been implicated in many aspects of RNA regulation, from protein synthesis to mRNA stability and decay. The literature on the fragile X related proteins' (FXPs) role in mRNA regulation and their potential mRNA targets is vast. Therefore, we developed an approach to investigate the function of FXPs in translational control using three potential mRNA targets. Briefly, we first selected top mRNA candidates found to be associated with the FXPs and whose translation are influenced by one or more of the FXPs. We then narrowed down the FXPs' binding site(s) within the mRNA, analyzed the strength of this binding in vitro, and determined how each FXP affects the translation of a minimal reporter mRNA with the binding site. Overall, all FXPs bound with high affinity to RNAs containing G-quadruplexes, such as Cyclin Dependent Kinase Inhibitor p21 and FMRP's own coding region. Interestingly, FMRP inhibited the translation of each mRNA distinctly and in a manner that appears to correlate with its binding to each mRNA. In contrast, FXR1P/2P inhibited all mRNAs tested. Finally, although binding of our RNAs was due to the RGG (arginine-glycine-glycine) motif-containing C-terminal region of the FXPs, this region was not sufficient to cause inhibition of translation.

Introduction

Fragile X Syndrome (FXS) is the predominant type of inherited intellectual disability and autism spectrum disorder, as well as the first genetic disorder to link RNA regulation to human cognitive function [1,2]. Patients with this disorder may experience seizures, hyperactivity, anxiety, and poor language development [1]. On a cellular level, patients with FXS possess a greater density of dendritic spines, and increased numbers of long and immature-shaped spines [3]. It is estimated that 1 in 5,000 males and 1 in 4,000 to 8,000 females possess the full FXS mutation [1]. FXS predominantly results from

*To whom correspondence should be addressed. Tel: 858-822-2957, sjoseph@ucsd.edu.

Contributions

All authors designed the experiments. M.E. performed the experiments, and all authors discussed the results. M.E. wrote the paper with input from S.J. S.J. supervised all aspects of the work.

Competing Interests

The authors declare no competing interests.

a CGG trinucleotide repeat expansion in the 5' untranslated region of the *FMR1* gene [1,4]. The expanded repeats are hypermethylated causing transcriptional silencing of the *FMR1* gene, leading to a deficiency or absence of fragile X mental retardation protein (FMRP) [1,4–6]. FMRP's role in RNA regulation and translation repression has been studied extensively, particularly as it relates to FXS [4]. Beyond FXS and autism spectrum disorder, genes of FMRP mRNA targets are enriched for psychiatric disorders: a recent article found genes with a high probability of being FMRP targets were enriched for association with schizophrenia, bipolar disorder, and major depressive disorder [7]. If we extend our discussion of RNA regulation to the entire fragile X protein family, the impacts of RNA misregulation on human health go beyond neuronal development and cognition.

FMRP is one of three RNA-binding, ribosome-associating proteins involved in translational regulation that comprise the fragile X protein (FXP) family; the other two members are referred to as fragile X-related protein 1 (FXR1P) and fragile X-related protein 2 (FXR2P) [8–11]. While less studied, FMRP's autosomal paralogs, FXR1P and FXR2P, are noteworthy for their role in translational regulation as their deficiency also leads to developmental abnormalities [8,9,12]. For example, FXR2P-deficient mice have impaired dendritic maturation of new neurons, with new neurons possessing shorter and less complex dendrites compared to wild-type mice [13]. These mice revealed decreased neural connectivity as new neurons with shorter dendrites connected to fewer presynaptic neurons [13]. On the other hand, FXR1P is unique among the FXPs as in humans, FXR1P mRNA demonstrates alternative splicing and is abundant in heart and skeletal muscle tissue [8,14–16]. Furthermore, FXR1P expression is altered in myoblasts from patients with facioscapulohumeral muscular dystrophy [15].

The FXPs are multidomain proteins with high amino acid identity over the first 58–70% of their sequences, but lower identity thereafter (Figure 1A) [17]. All three proteins possess RNA-binding domains of interest: three K homology (KH) domains within the highly conserved N-terminal region, and an arginine-glycine-glycine (RGG) motif with poor conservation located in the divergent C-termini (Figure 1B–D) [12,18,19]. In addition, all three proteins possess two Agenet domains which have been shown to bind methylated lysines [20,21]. A less explored feature of the FXPs is their C-terminal intrinsically disordered region (IDR) which constitutes ~30–43% of the entire protein sequence but has lower sequence conservation (Figure 1A) [17]. IDRs are enriched in RNA-binding proteins compared to the entire human proteome and can support protein aggregation, phase transitions, and bind to RNA both specifically and non-specifically [22,23]. Within the IDR of FXR1P and FXR2P are arginine-rich motifs that likely impart these paralogs with unique RNA-binding capabilities. The isoform of FXR1P that we study, isoform 2, has one such region, while FXR2P has two. Due to their similarity to the nucleolar-targeting signal (NoS) of the protein Rev of human immunodeficiency virus type 1, these sequences are referred to as NoS1 and NoS2 respectively [24]. In other proteins, these motifs have been shown to support RNA recognition, where the few non-arginine amino acids mediate specific binding [25].

Many studies have attempted to identify and validate the mRNA targets of FMRP, while several papers have identified targets of FXR1P and FXR2P [13,26–32]. Although there

appears to be overlap in the mRNA targets of the FXP family, there is evidence that each protein has unique mRNA targets [12,13,26,29,31,33]. To validate, analyze, or compare the mRNA targets of the FXP family determined from pull-down methods, researchers often test the direct binding of each protein to its mRNA targets in vitro. These studies allow researchers to identify binding sites within a target mRNA or test binding to in vitro selected RNAs, which can lead to the identification of sequence motifs or structural features the proteins may recognize in vivo [34–36]. Such studies have identified G-quadruplexes and kissing complexes as RNA features recognized by FMRP [12,34–36].

One immense challenge to determining the mRNA targets of FMRP has been confounding influences such as the biological material or cell type used for assays, the assay implemented, the analyses applied, the presence of FXP interaction partners, and even the particular isoform of the FXP, to name just a few [26]. As just one example, it has been reported that FXR1P can either repress or activate translation of its target mRNAs in non-neuronal cells depending on the cellular context, while different isoforms of FXR1P appear to inhibit translation through distinct mechanisms such as destabilizing mRNA transcripts or through regulating the process of translation itself [30,37]. In an attempt to disentangle our understanding of FMRP's mRNA targets, Suhl *et al.* performed a comparison of three large FMRP mRNA target studies and found an overlap of only ~3.2%, indicating that the methods used significantly impacted the results [26]. From this overlap between three FMRP mRNA target studies (Brown, Darnell, and Ascano-RIP), Suhl *et al.* provided a list of the top 40 targets of FMRP that are associated with FXS, autism, and mental retardation/intellectual disability [26]. Despite the many confounding factors clouding research into FXS therapeutics, by identifying an enriched FMRP recognition motif (WGGA clusters that could form G-quadruplexes), as well as top targets shared amongst three unique studies, Suhl *et al.* provided researchers with a place to focus their attention for therapeutic targets [26].

To further investigate reporter mRNA targets of the FXPs, we developed a method to authenticate the numerous targets identified in vivo or through pull-down assays and the few targets worth pursuing for therapeutics (Figure 2A). First, we narrowed our focus to the most biologically relevant target RNAs with which one or more of the FXPs have been shown to (1) interact with through RNA pull-down assays, (2) exert an influence over in vivo, and (3) contain potential G-quadruplexes (Figure 2B). We then validated and quantified direct binding of the FXPs to these RNAs in vitro by determining binding affinities using a fluorescence anisotropy assay. At this stage we confirmed that the targets are capable of forming G-quadruplexes with an N-methyl mesoporphyrin IX (NMM) assay [38]. The validated candidates (and corresponding negative controls) were then incorporated into our minimal reporter mRNA to observe if translation was altered in the presence of the FXPs (Figure 2C). Our systematic studies revealed that FMRP, FXR1P, and FXR2P all bind with high affinity to G-quadruplex RNAs. Interestingly, FMRP inhibited translation of our minimal reporter mRNA with the P21 γ G-quadruplex, whereas FXR1P/2P inhibited translation independent of G-quadruplex structures in the mRNA. Thus, FMRP's translation inhibition correlated with its mRNA binding affinity, whereas FXR1P/2P inhibited translation independently of their mRNA binding affinities.

Results

The mRNA targets of the FXPs have been identified by RNA pull-down assays, such as cross-linking immunoprecipitation (CLIP), which report RNA-protein interactions that may not have a strong initial interaction, and may not be physiologically relevant [26]. Such errors can be introduced through the crosslinking method utilized, particularly as the specificity of crosslinking is not fully understood [26,39]. This problem is prevalent as many studies have reported results with little overlap and have identified few targets with a validated association with FMRP [26]. For the initial testing of our approach, we further narrowed our focus to two targets: G-quadruplexes and AU-rich regions. We selected mRNAs that possess the potential to form G-quadruplexes as this structure has steadfastly been reported as a target of FMRP, and we have recently shown it is a target of the entire FXP family [12,17,35,36,40]. A very recent study supports our decision to focus on G-quadruplexes: mRNA transcripts in FMRP-null mouse neuronal cells that depend on FMRP for efficient transportation in neuronal cells were enriched for G-quadruplex sequences in their 3’ UTRs; similar results were also observed in the neurons derived from FXS patients [41]. Additionally, FMRP has been found to bind to G-quadruplexes in both the 5’ and 3’ UTRs of its target mRNAs, often as a means to inhibit their translation [42]. Second, we selected an AU-rich region, as this was a reported target of FXR1P [31,41,42].

For our biologically relevant RNA targets we selected the G-quadruplex forming regions of Cyclin Dependent Kinase Inhibitor p21 (P21 γ) and FMR1 (N19) mRNAs from previous publications, as well as the AU-rich region of Tumor Necrosis Factor α (TNF-α) (Figure 2B) [30,31,36,43,44]. P21 γ was discovered when Davidovic *et al.* searched for mRNA targets of FXR1P that could be linked to the extreme muscular phenotypes that are observed in FXR1P’s absence [30]. They observed that the cell-cycle progression regulator p21 was increased in Fxr1 knockdown Facio-Scapulo Humeral Dystrophy human myoblasts leading to premature exit of the cell-cycle [30]. Furthermore, FXR1P was found to bind p21 mRNA through a G-quadruplex in its 3’ UTR (referred to as P21 γ), with the FXR1P/G-quadruplex complex leading to a reduced half-life of the p21 mRNA [30]. For our P21 γ RNA sequence we reduced their P21 γ sequence to the nucleotides listed as 918–955 of murine Cyclin Dependent Kinase Inhibitor p21 as reported in Davidovic *et al.* [30]. To create a negative control RNA which we refer to as Mutant γ, we simply replaced all the guanines in our P21 γ sequence with cytosines, which precludes the formation of G-quadruplexes in Mutant γ.

The second G-quadruplex of interest, referred to as N19, is located within the coding region of FMRP’s own mRNA [36]. FMRP was found to bind to a 100-nucleotide region that codes for FMRP’s RGG motif with a specific and high affinity interaction [36]. Additionally, when this region was inserted into the 5’ UTR of a reporter gene, FMRP inhibited its translation, leading researchers to question if FMRP negatively regulates its own expression in vivo [36]. From this publication, we selected a portion (38 nucleotides of the 100-nucleotide region) of Human FMRP’s mRNA that was reported to be necessary but not sufficient for FMRP’s binding [36]. FMRP was originally believed to inhibit its own translation by binding to this region; however, a follow-up study revealed that *FMR1* mRNA G-quadruplexes are potent exonic splicing enhancers [42,45]. It appears that the binding of FMRP to G-quadruplexes within its mRNA regulates the production of different isoforms of FMRP [42,45]. It is

important to note that an additional study found that FXR1P (only the long isoform e) was also able to bind to this RNA specifically [46].

Finally, we selected the 3' UTR AU-rich element (ARE) of Human TNF-α which is highly conserved among mammals [43]. In fact, the region is so conserved that we were able to select a portion that was present in all three papers we reviewed on this mRNA [31,43,44]. All three articles cite this mRNA as a target of FXR1P, with two reporting that FXR1P represses TNF-α translation [31,43,44]. As we had selected three biologically relevant mRNAs that (1) are bound by one or more of the FXPs, and (2) whose translation are regulated by one or more of the FXPs, we were able to move to the next step of our analysis.

Since we had reduced the mRNA target sequences to 37 (ARE) or 42 nucleotides (P21 γ, Mutant γ, & N19), we first used QGRS mapper and RNAfold to confirm that our reduced G-quadruplex sequences were still predicted to form G-quadruplex structures [47,48]. Once we had synthesized these RNAs, we used an N-methyl mesoporphyrin IX (NMM) assay to detect G-quadruplex formation and found that our P21 γ and N19 sequences were capable of forming G-quadruplexes [38] (Figure 3A–B). It is worth mentioning that the P21 γ G-quadruplex appears very stable, as it can form even after refolding in the presence of LiCl.

We subsequently utilized fluorescence anisotropy assays to determine if our RNAs were still bound by the FXPs, and to rank the FXPs binding affinity for each RNA by determining equilibrium dissociation constants (K_D values) (Figure 3C–E). This step proved essential, as we found binding to the AU-rich region of Tumor Necrosis Factor-α was much weaker than for the G-quadruplex RNAs, and thus a less ideal RNA for our in vitro translation studies, or as a therapeutic target (Supplemental Figure 1). However, we obtained binding affinities similar to those reported in the literature (0.96 μM), bolstering our confidence in our methods (data not shown) [44]. Additionally, the FXPs showed little to no binding to the Mutant γ sequence, making it a potential negative control RNA. After this step, we narrowed our focus to the G-quadruplex targets, P21 γ and N19, as the binding affinities of the FXPs for these RNAs were much stronger than for the ARE.

When assessing a potential mRNA target of FMRP, or its paralogs, researchers (including our own lab) have often added the target mRNA sequence into the 5' or 3' (UTRs) of reporters such as *Renilla,* firefly or NanoLuc luciferases [30,36,43,49]. However, the use of large reporter RNAs can convolute the interpretation of data from in vitro translation experiments (IVT), impairing the ability to specifically determine if a protein's association with the target mRNAs alters their translatability. With the length of these reporters (NanoLuc – 557 nucleotides, *Renilla* – 997 nts, and firefly – 1702 nts) comes an increasing probability for the presence of a FMRP target RNA sequence or motif located within the reporter itself. Especially alarming is the fact that our bioinformatic analysis indicates that all the luciferases' mRNA sequences possess potential G-quadruplex forming sites, (NanoLuc- 3, *Renilla* – 3, and firefly – 5) a well-recognized RNA structural target of FMRP. Moreover, preliminary data from our lab corroborates that the FXPs can bind to the reporters themselves. Although researchers may attempt to control for such binding sites, we preferred to create a minimal reporter mRNA (118 nucleotides), to reduce the chance of extraneous

binding sites occurring within the mRNA and to eliminate potential G-quadruplex formation sites.

We incorporated our target and control RNA sequences into the 3' UTR of our minimalistic reporter mRNA and added a 5' methylguanosine cap, a Kozak sequence, and a 30 nucleotide 3' poly(A) tail to mimic a eukaryotic mRNA (Figure 2C). We also created a control reporter that lacks a 3' UTR sequence. Each reporter mRNA encodes a FLAG peptide which allows for purification from other proteins in our system, and several methionines, which enable detection. The design of our reporter was influenced by other research groups who have had success monitoring the translation of a small reporter RNA [50,51]. However, in contrast to these groups, we found more success monitoring the production of our peptide through radiolabeling, as opposed to immunoblot analysis [50,51]. We refer to our minimalistic reporter RNAs as NanoFX mRNAs.

After creating our NanoFX mRNAs, we verified that the 5' capping step was successful by ensuring that eIF4E bound these NanoFX mRNAs (Supplemental Figure 2A). We also verified that the G-quadruplexes could still form within the context of a NanoFX mRNA using the NMM assay. Indeed, both P21 γ and N19 NanoFX mRNAs formed G-quadruplex structures (Supplemental Figure 3A). Next, we confirmed the FXPs' ability to bind the target sequences within the context of a NanoFX mRNA by EMSAs. For the NanoFX mRNAs, we observed a similar binding affinity trend to that from our fluorescence anisotropy assays: tightest binding to the P21 γ NanoFX mRNA, followed by the N19 NanoFX mRNA, with similar or perhaps lower binding to the Mutant γ version, and no binding to our NanoFX mRNA with no 3' UTR (Figure 4A–C). The two bands present in each lane of this native gel represent the folded RNA monomers to which the FXPs bind (shifted further), and an intermolecular dimer (present close to wells) (see Supplemental Figures 2B–C). Interestingly, we found that for the N19 NanoFX mRNA, refolding appears to lead to increased binding by FMRP, which is likely true for all the FXPs (Supplemental Figure 3B). This suggests that refolding may need to occur for the G-quadruplex to form within the N19 NanoFX mRNA. On the other hand, the P21 NanoFX mRNA was bound similarly by FMRP regardless of refolding. We subsequently proceeded to test our NanoFX mRNAs in our IVT assay, making sure to refold the N19 NanoFX mRNA prior to this assay.

Translation efficiency of the NanoFX mRNAs in the presence vs. absence of the FXPs was assessed by tracking incorporation of ^{35}S-methionine into the resulting peptide. We performed our IVT reactions in rabbit reticulocyte lysate (RRL) lacking methionine (-MET), then isolated the peptide from other proteins within the system using anti-FLAG M2 beads. The translation efficiency was quantified by liquid scintillation counting and visualized by phosphorimaging (Figure 5A). Overall, we observed different trends for FMRP compared to its paralogs, FXR1P and FXR2P (Figure 5B–D). While FMRP regulated each NanoFX mRNA distinctly, and in a manner that appears to correlate with its binding to each NanoFX mRNA, FXR1P/2P inhibited all NanoFX mRNAs tested. Whereas FXR1P appeared to inhibit each NanoFX mRNA to a similar extent, FXR2P inhibited the P21 γ NanoFX mRNA the most. This data suggests that FMRP may function as a specific regulator of translation, whereas FXR1P/2P may, at least in some contexts, function as global translation regulators.

To further investigate how the FXPs regulate mRNAs in vitro, we tested the translation of the P21 γ NanoFX and no 3' UTR NanoFX mRNAs the presence of lower quantities of protein. Our titration revealed that all three FXPs appear to inhibit the translation of the P21 NanoFX in a concentration dependent manner, with the greatest inhibition at 500 nM FXPs. The highest concentration we tested was 500 nM FXPs as this is a biologically relevant concentration and due to the limitations of our chosen system (Supplemental Figure 4A–C). For instance, although we controlled for the addition of reagents to our system, RRL is inhibited by addition of excessive salt, and the FXPs must be stored in high salt storage buffers, precluding us from testing higher protein concentrations. For the no 3' UTR NanoFX, inhibition was seen at higher concentrations, but we did not observe a continual decrease of inhibition as more protein was added.

Next, we tested how the FXPs regulate translation during our assay by performing a time course assay. We compared the FXPs' regulation to a protein control, maltose-binding protein (MBP), a protein we have previously demonstrated does not bind RNA or regulate translation [17]. Samples taken at various time points throughout the assay revealed that translation of the P21 NanoFX reporter occurs continually in the presence of all proteins tested (Supplemental Figure 5A). For all reactions, the amount of peptide being produced increases throughout the experiment, with the rate of production slowing towards the end of the experiment. After 50 minutes, the scintillation counts remain constant or begin to decline for all samples. To further validate our results, we also performed a time course to analyze the regulation of *Renilla* luciferase mRNA, an mRNA we have previously demonstrated is inhibited by the FXPs, but not MBP [17]. In this assay, we compared translation in the presence of the FXPs to MBP and to each protein's respective buffer: the FXPs clearly inhibited translation with respect to their buffer controls, whereas MBP did not (Supplemental Figure 5B). Although the production of protein increased over time for all samples, there was significantly less protein produced at each time point with the FXPs compared to MBP or their buffer controls.

Finally, we tested whether the addition of the FXPs leads to degradation of the no 3' UTR and P21 γ NanoFX mRNAs in RRL by purifying the mRNA from the RRL system after incubation. Although we previously observed that the FXPs generally reduce the translation of the NanoFX mRNAs compared to their buffer controls, we did not observe degradation in the presence of the FXPs for either NanoFX mRNA (Supplemental Figure 6). We therefore conclude that the inhibition we observed in our system is not due to degradation of the NanoFX mRNAs. Overall, our IVT experiments were successful for determining how the FXPs regulate each mRNA target sequence in vitro without the influence of other RNA recognition elements (obvious or cryptic) that are present in the larger luciferase reporters.

For the final part of our study, we were curious how the different RNA-binding domains of the FXPs contribute to the proteins' ability to bind and regulate our mRNA targets. Many in vitro studies of FMRP have focused on only a section of this protein, as the full-length protein is challenging to purify, so we were also interested in comparing the results of the full-length protein to those of its RNA-binding domains. As the KH domains and the RGG motif of FMRP have been of primary interest to researchers, we decided to focus on the KH0-KH2 domains and the RGG motif through C-terminal end of FMRP (Figure 6A).

From our fluorescence anisotropy assays, we were not surprised to find that the RGG motif of FMRP was able to bind RNA sequences whereas the KH domains were not (Figure 6B). This aligns with the plethora of research demonstrating that the RGG motif binds to G-quadruplex structures [40,41]. However, when comparing the binding affinities of the RGG motif to full-length FMRP, we observed greatly reduced binding for the RGG motif. Thus, other regions of FMRP must contribute to its RNA-binding ability, perhaps the region between the KH domains and the RGG motif that was not included in either of our constructs but is present in the full-length protein.

The fluorescence anisotropy binding data were consistent with our binding studies with the NanoFX mRNAs. Again, the KH domains did not bind to either of the NanoFX mRNAs tested while the RGG motif bound to the G-quadruplex P21 γ NanoFX mRNA, yet not as tightly as the full-length protein (Figure 6C). When testing the effect of these constructs on in vitro translation, we observed that the RGG motif did not inhibit the NanoFX mRNA with no 3’ UTR (Figure 6D). This aligns with the fact it did not bind this NanoFX mRNA and is consistent with the results for full-length FMRP. The RGG motif only slightly inhibited the P21 γ NanoFX mRNA, even at 1 μM protein concentration, which is double the protein concentration used for the studies with full-length FMRP. The KH domains did not inhibit the P21 γ NanoFX mRNA as predicted, but we observed some inhibition for the no 3’ UTR NanoFX mRNA. Since the full-length FMRP did not inhibit the no 3’ UTR NanoFX mRNA, this suggests it is ideal to analyze the function of the full-length protein whenever possible, as this should yield the most biologically relevant results. Nevertheless, our studies with the KH domains and RGG motif yielded useful insight into individual contributions to the full protein’s function: the RGG motif was responsible for binding G-quadruplex RNAs yet was unable to lead to the same levels of inhibition as observed for the full-length protein. Thus, the various domains in FMRP must cooperate to inhibit the translation of its mRNA targets.

Discussion

Our studies show that G-quadruplexes within biologically relevant mRNAs P21 γ and N19 are bound by all FXPs with high affinity: equilibrium dissociation constants (K_D) in the nanomolar range. We confirmed that the FXPs still bound these target sites within the NanoFX mRNAs before testing them in our IVT system. Both FMRP and FXR2P have the highest binding affinity for P21 γ mRNA and exert the greatest influence over its translation in the context of a NanoFX mRNA. Additionally, refolding the P21 γ NanoFX mRNA does not seem to greatly influence FMRP’s ability to bind this RNA, perhaps because it forms a more stable G-quadruplex structure. Thus, of the two target RNA targets that we analyzed, P21 γ appears to show the greatest potential for therapeutics. As FMRP reduced P21 γ’s translation, this suggests researchers could investigate inhibitors of the cell-cycle regulator Cyclin Dependent Kinase Inhibitor p21 (*p21*) as a treatment to reverse the effects of FXS. Our results support previous researchers’ speculations that an excess of *p21* due to a lack of FMRP may lead to errors in p21-dependent cell cycle exit of neuronal progenitors during neurogenesis [52].

Our research also provided us with further insight into the differences between each of the FXPs. For example, our finding that FMRP may regulate mRNAs in a manner distinct from

the other FXPs has led us to question whether the R-rich regions present only in FXR1P/2P lead to enhanced or less specific RNA-binding and inhibition (Figure 7). Interestingly, while studies have reported that only the long, muscle specific isoforms of FXR1P can bind to G-quadruplexes, we did not find this to be true [46]. Our neuronal Human isoform 2/b of FXR1P bound to and regulated the translation of G-quadruplex NanoFX mRNAs. In line with previous research where FXR1P was found to preferably bind to a G-quadruplex over an AU-rich region within the 3' UTR of P21 mRNA, we observed the same RNA-binding preferences for FMRP and FXR1P in our studies as well (FXR2P was not tested with AU-rich RNA, although we predict it would behave similarly) [30].

We further analyzed the functions of the KH domains and RGG motifs, which drew our attention to potential new avenues of research. By comparing the functions of FMRP to its KH domains and RGG motif, we found that the RGG motif appears to be predominantly responsible for FMRP's binding to G-quadruplexes, yet other regions of the protein must contribute to the greatly increased binding affinity of the full-length protein, and its greater translation inhibition. Therefore, it would be interesting to investigate contributions that the region between the KH domains and RGG motif make to the overall protein's function. In agreement with this finding, previous work in our lab demonstrated that the C-terminal region of FMRP plays an essential role in the inhibition of translation, yet an N-terminally truncated FMRP led to greater inhibition [49]. This result, corroborated by our findings, indicates that the unstructured region between the KH domains and the RGG motif, may cooperate with the RGG motif/C-terminus of FMRP to regulate translation [49]. Another possibility is that the RNA-binding capabilities of the RGG motif are augmented by the FXPs' ability to dimerize. As the ability of the FXPs to dimerize has been attributed to their N-terminal regions, this could explain why our RGG motif construct bound RNA and inhibited translation, but not to the same extent as full-length FMRP [53].

A second interesting finding was that the KH domains did not bind any RNAs we tested, however, we cannot rule out the possibility that the KH domains can bind RNA sequences or structures not tested in this study. We also observed slight translation inhibition of our no 3' UTR NanoFX mRNA by the KH domains, leading us to consider that they may support the overall function of the full-length FXPs in inhibiting translation. Our findings support using the full-length versions of these proteins in vitro to gain a more thorough understanding of their biological functions. We have previously published a method to purify the full-length versions of all the FXPs, so researchers may now easily and accurately test how FMRP and its paralogs behave, which have been shown to be important for proper neural, muscle, and cardiac development as described previously [17].

Our work also provided insight into the stability of the RNA structures we tested. We were able to shorten the G-quadruplex targets to 42 nucleotide sequences, and still observed high affinity binding and translation inhibition. Furthermore, we observed that in contrast to N19, the G-quadruplex in P21 γ appears to be very stable, forming even after refolding in the presence of LiCl. The sensitivity of the N19 G-quadruplex structure may explain why Schaeffer *et al.* found that their 35 nucleotide sequence was necessary but not sufficient for FMRP's binding, whereas we were able to get binding with only 38 out of the 100 nucleotides from their reported functional binding site [36]. Interestingly, we observed

that FMRP appeared to bind the N19 NanoFX mRNA more tightly after a refolding step. In line with this finding, all FXPs had a slight inhibitory effect on the N19 NanoFX mRNA after a refolding step (Supplemental Figure 3C). This finding indicates that the FXPs regulatory effects may, in certain situations, depend on the structure of the RNA in question. Additionally, the fact that the FXPs did not inhibit N19 NanoFX mRNA without refolding demonstrates that reagents from our protein purification were not the cause of the observed inhibition of translation. It is tempting to speculate, and future studies may wish to address, whether the folded state of a G-quadruplex RNA is a mechanism through which the cell controls how an mRNA should be regulated. Recent work has demonstrated that G-quadruplexes can function as regulatory elements in neurological disorders, and thus may themselves serve as effective therapeutic targets for FXS and other disorders [42].

Finally, our results illustrate how our approach can yield valuable information for FXS therapeutics (or other disorders). As researchers pursue costly and lengthy therapeutics, many seemingly viable targets for FXS treatments will not meet the necessary standards. It is therefore imperative that biochemists continue performing stringent assays to validate the overabundance of potential FMRP targets identified from RNA pull-down assays. Such validations will refine our list of potential targets, providing researchers with greater chances of success in identifying treatments for FXS.

Materials & Methods

Purification of Fragile X Proteins

The fragile X proteins (FMRP, FXR1P, & FXR2P) were purified as described previously using KCl as the salt in elution buffers [17]. A step gradient of KCl was used instead of a linear gradient to elute the fragile X proteins. The FMRP KH0-KH2 domains and the RGG motif were purified by Youssi Athar as described previously [38].

In vitro Transcription of P21 γ, Mutant γ, & N19 RNAs and NanoFX mRNAs

Oligos containing a T7 promoter sequence were ordered from Integrated DNA Technologies (IDT). Oligos for the short 3’ UTR sequences were first gel purified, then annealed to the 18T7T primer prior to transcription reactions. Oligos for the NanoFX mRNAs (except for the no 3’ UTR NanoFX mRNA) were PCR amplified prior to transcription.

For each 100 μL transcription reaction the following reactants were used: 1000 pmol of oligo annealed to 1000 pmol 18T7T primer (for the 3’ UTR sequences and no 3’ UTR NanoFX mRNA) or 10 μL of the PCR-generated DNA template (for the three NanoFX mRNAs with a 3’ UTR), 4 mM NTPs, 1X transcription buffer (40 mM Tris pH 8.0, 20 mM $MgCl_2$, 2 mM Spermidine, 0.1% Triton X-100), 5 mM DTT, and ~ 0.27 μg of T7 RNA polymerase. Each reaction was treated with 2 units of RQ1 DNase (Promega) for 30 min at 37 °C, followed by gel purification on 15% denaturing polyacrylamide gels.

DNA Templates to Produce Target RNA Sequences—All DNA templates to produce the target RNA sequences were transcribed using the 18T7T primer: 5’-TAATACGACTCACTATAG-3’

P21 γ: 5’-
ACCCCATCCCAGATAAGCCCACCCCCACCACCACACACCCCCTATAGTGAGTCGTATTA-3’

Mutant γ: 5’-
AGGGGATGGGAGATAAGGGGAGGGGGAGGAGGAGAGAGGCCCTATAGTGAGTCGTATTA-3’

N19: 5’-
AGAAGCCTCCTCCACGTCCTCTTCCTCCTTGTCCTCTTCCCCTATAGTGAGTCGTATTA-3’

ARE: 5’-
TAAATAAATAAATAATAAATAAATAATAAATAATCCCTATAGTGAGTCGTATTA 3’

Resulting Target RNA Sequences

P21 γ: 42 nucleotides 5’-
GGGGGUGUGUGGUGGUGGGGGUGGGCUUAUCUGGGAUGGGGU-Fluorescein-3’

Mutant γ: 42 nucleotides 5’-
GGGCCUCUCUCCUCCUCCCCCUCCCCUUAUCUCCCAUCCCCU -Fluorescein-3’

N19: 42 nucleotides: 5′-
GGGGAAGAGGACAAGGAGGAAGAGGACGUGGAGGAGGCUUCU-Fluorescein-3′.

ARE: 37 nucleotides 5’-GGGAUUAUUUAUUAUUUAUUUAUUAUUUAUUUAUUUA-Fluorescein-3’

DNA Templates to Produce NanoFX mRNAs

No 3’ UTR NanoFX mRNA: 5’-
TTTTTTTTTTTTTTTTTTTTTTTTTTTTTTTTTACATCATCATATCGCCGTCATGGTCTTTGTAGTCCATGGTGGCGGCCTATAGTGAGTCGTATTA-3’

P21 γ NanoFX mRNA: 5’-
ACCCCATCCCAGATAAGCCCACCCCCACCACCACACACCTTACATCATCATATCGCCGTCATGGTCTTTGTAGTCCATGGTGGCGGCCTATAGTGAGTCGTATTA-3’

Mutant γ NanoFX mRNA: 5’-
AGGGGATGGGAGATAAGGGGAGGGGGAGGAGGAGAGAGGTTACATCATCATATCGCCGTCATGGTCTTTGTAGTCCATGGTGGCGGCCTATAGTGAGTCGTATTA-3’

N19 NanoFX mRNA: 5’-
AGAAGCCTCCTCCACGTCCTCTTCCTCCTTGTCCTCTTCTTACATCATCATATCGCCGTCATGGTCTTTGTAGTCCATGGTGGCGGCCTATAGTGAGTCGTATTA-3’

Primers to PCR the NanoFX mRNA DNA templates and add a 30-nucleotide Poly-A Tail—All NanoFX mRNAs with 3’ UTRs were made using the same forward primer: 5’-TAATACGACTCACTATAGGC-3’

Reverse primers:

P21 γ NanoFX mRNA Reverse Primer: 5’-TTTTTTTTTTTTTTTTTTTTTTTTTTTTTTACCCCATCCCAGATAAGC-3’

Mutant γ NanoFX mRNA Reverse Primer: 5’-TTTTTTTTTTTTTTTTTTTTTTTTTTTTTTAGGGGATGGGAGATAAGG-3’

N19 NanoFX mRNA Reverse Primer: 5’-TTTTTTTTTTTTTTTTTTTTTTTTTTTTTTAGAAGCCTCCTCCACGTC-3’

The NanoFX mRNA without a 3’ UTR was produced through transcription after annealing with the 18T7T primer: 5’-TAATACGACTCACTATAG-3’

3’ Fluorescein Labeling of P21 γ, Mutant γ, & N19 RNAs and NanoFX mRNAs

RNAs used for fluorescence anisotropy, EMSAs, and mRNA stability experiments were 3’ labeled with fluorescein as described below.

To label the RNA, 0.5 nmoles of RNA was 3′ oxidized for 90 min at room temperature (100 mM KIO_4, 100 mM NaOAc pH 5.2) then incubated with fluorescein 5-thiosemicarbizide (FTSC) at 4 °C overnight (100 mM NaOAc pH 5.2, 1.5 mM FTSC). The RNA was then purified using a Monarch RNA Clean-up Kit (New England BioLabs).

5’ Capping of NanoFX mRNAs with Vaccinia Capping Enzyme

To mimic a mammalian mRNA, the NanoFX mRNAs with 3’ poly(A) tails were 5’ capped as follows.

Pure RNA was denatured by heating at 65°C for 5 minutes and refolded by cooling on ice for 5 minutes. Each 50 μL reaction consisted of 1X Capping Buffer (New England Biolabs), 0.5 mM GTP, 0.1 mM S-adenosylmethionine (New England Biolabs), Vaccina capping enzyme (0.24 μg/10 μg of RNA for RNAs >100 nucleotides), RNA (~ 20–30 μg), and water. Each reaction was incubated at 37°C for 2 hours then purified using a Monarch RNA Clean-up Kit (New England BioLabs).

Successful capping was verified by testing the binding of 250 nM of eukaryotic initiation factor 4E (eIF-4E) to 50 nM of each 3’ fluorescein labeled NanoFX mRNA using an electrophoretic mobility shift assay on a 0.6% native agarose gel run in 1X TBE for 75 min at 66V.

N-methyl mesoporphyrin IX (NMM) assay to detect G-quadruplex formation

A stock solution of NMM (Frontier Scientific) was prepared as previously described [38]. The stock solution of NMM (8.61 mM in 0.2 N HCl) was diluted to 400 μM in 10% (v/v) DMSO to make a fresh working solution. Each RNA was refolded in the presence of KCl

and LiCl (50 mM Tris pH 7.5, 2 mM $MgCl_2$, 75 mM KCl or LiCl). For 3' UTR sequences, 4 μM of RNA was used; for the NanoFX mRNAs, 2 μM of RNA was used. Refolding occurred for 5 min at 68°C followed by slow cooling to room temperature for ~1 hr. After cooling, 2 μL of 400 μM NMM solution was added to 160 μL of refolded RNA to achieve a final concentration of 5 μM NMM (1.25 μL to 100 μL for the NanoFX mRNAs). The samples were then incubated at room temperature for 10 min prior to loading 155 μL (90 μL for the NanoFX mRNAs) of each sample into a 96-well non-binding plate (Greiner Bio-One) for a fluorescence intensity scan using a multimode microplate reader (SPARK TECAN). The samples were excited at 400 nm and the emission scanned at 560–650 nm with 5 nm bandwidths for both excitation and emission. The fluorescence intensity values were plotted as a function of wavelength from 580–640 nm. Two trials were performed for each RNA (n=2).

Assessing RNA-binding of the Fragile X Proteins through Fluorescence Anisotropy

Prior to fluorescence anisotropy assays, each protein stock was thawed from −80°C then centrifuged at 16,100 RCF, 10 min, 4 °C with a benchtop centrifuge to remove any precipitated protein prior to each experiment. The supernatants containing soluble protein were obtained and the concentration of protein determined using A280 readings (Thermo Scientific NanoDrop 2000/2000c spectrophotometer). RNAs labeled with a 3′ fluorescein were diluted to 5X concentrations (~ 25 nM). The RNAs in these 5X solutions were renatured in renaturation buffer (50 mM Tris pH 7.5, 75 mM KCl, 2 mM $MgCl_2$) by heating at 68 °C for 5 min, then slow cooled from 68 °C to ~ 28 °C for ~ 1 h in a water bath. Water, binding buffer, protein storage buffer, protein, and the 5X RNA solution were added in the order listed and mixed for a final reaction volume of 200 μL. The final reactions contained 20 mM Tris pH 7.5, 75 mM KCl, 5 mM $MgCl_2$, 1 μM BSA, 1 mM DTT, 100 ng/μL tRNA (to prevent non-specific binding), and ~ 5 nM RNA. Various concentrations of protein were added for each protein to create a titration curve. It is important to note that for each protein concentration tested the total volume of protein + protein storage buffer remained constant. In each trial the binding buffer was adjusted to account for the Tris pH 7.5 and DTT that were contributed from the protein storage buffer. Reactions were thoroughly mixed and incubated in the dark at room temperature for 1 h. After incubation, each reaction was added into a 96-well non-binding plate (Greiner Bio-One) for fluorescence anisotropy using a multimode microplate reader (SPARK TECAN). Samples were excited at 485 nm and emission was measured at 535 nm. To determine binding affinities, the anisotropy data from each binding assay were normalized to initial values without protein, plotted, and fit to a quadratic equation as previously described [38]. At least three independent trials (n=3) were performed to determine standard deviations for all proteins except for at 9000 nM for Mutant γ for the C-terminus of FMRP for which only two trials were performed. If applicable, outliers (significance level set as 0.05) were removed.

RNA-binding of Fragile X Proteins by Electrophoretic Mobility Shift Assay

To confirm the proteins could still bind to the P21 γ and N19 sequences within the context of the NanoFX mRNAs, the binding of each protein to the 3' fluorescein labeled NanoFX mRNAs was tested through an electrophoretic mobility shift assay. This assay was used as the NanoFX mRNAs are too large to be compatible with fluorescence anisotropy assays.

The purified proteins were centrifuged at 16,100 RCF, 10 min, 4 °C with a benchtop centrifuge to remove any precipitated protein prior to each experiment. The supernatants containing soluble protein were obtained and the concentration of protein determined using A280 readings (Thermo Scientific NanoDrop 2000/2000c spectrophotometer). Fluorescein-labeled NanoFX mRNAs were diluted to 10X concentrations (1 μM) in water. For the RNA refolding assays only, the 1 μM RNA solutions were made in 50 mM Tris pH 7.5, 75 mM KCl, and 2 mM $MgCl_2$ and RNAs were refolded for 5 min at 68°C followed by slow cooling in a water bath to ~ 28 °C for ~ 1 h. Water, 10X binding buffer, protein storage buffer, proteins, and the 10X RNA solution were added in the order listed and mixed for a final reaction volume of 26 μL. The final reactions contained 50 mM Tris pH 7.5, 135–150 mM KCl, 5 mM $MgCl_2$, 1 μM BSA, 10 mM DTT, 50 ng/μL tRNA (to prevent non-specific binding), ~ 100 nM fluorescein-labeled RNA, and for reactions containing protein, 100–1000 nM of protein. For each protein concentration tested the total volume of protein + protein storage buffer remained constant. In each reaction the binding buffer was adjusted to account for the Tris pH 7.5, KCl, and DTT that were contributed from the protein storage buffer. The reactions were thoroughly mixed and incubated in the dark at room temperature for 1 h. After incubation, 3 μL of loading dye (xylene cyanol in 50% glycerol) was added to each reaction. A 0.8% native agarose gel (SeaKem GTG agarose) was prepared in 1X TBE buffer (100 mM Tris pH 8.3, 100 mM borate, 2 mM Na_2EDTA). After loading 13 μL of each sample, the gel was run at 4 °C for 2 h at 66 V in 1X TBE buffer. The gel was then scanned using a laser scanner (Typhoon FLA 9500, GE Healthcare) and the gel was analyzed in ImageJ.

Analysis of in vitro Translation Regulation of NanoFX mRNAs by the Fragile X Proteins

The purified proteins were centrifuged at 16,100 RCF, 10 min, 4 °C with a benchtop centrifuge to remove any precipitated protein prior to each experiment. The supernatants containing soluble protein were obtained and the concentration of protein determined using A280 readings (Thermo Scientific NanoDrop 2000/2000c spectrophotometer). For the N19 NanoFX mRNA only, prior to setting up the reactions, the RNA was refolded in renaturation buffer (50 mM Tris pH 7.5, 75 mM KCl, 2 mM $MgCl_2$) by heating at 68 °C for 5 min, then slow cooled from 68 °C to ~ 28 °C for ~ 1 h in a water bath. 2X rabbit reticulocyte lysate (treated with micrococcal nuclease to reduce endogenous mRNAs and without methionine), water, 5′ capped NanoFX mRNAs with a 30-nucleotide 3′ poly(A) tail, protein storage buffer, the corresponding protein, and L-[^{35}S]-Methionine (PerkinElmer, 10mCi (370MBq), Specific Activity: >1000 Ci (37.0 TBq)/mMole, 50 mM Tricine, 10 mM BME), were combined in the order listed, mixed, and allowed to incubate for ~75 min at 30°C. For time trial reactions, samples were taken from a master reaction at 0, 15, 30, 50, and 75 min. The final 20 μL reactions contained 100 nM NanoFX mRNA mRNA and 500 nM protein. For titrations, protein concentrations of 50, 100, 250, and 500 nM were tested. Higher concentrations could not be tested due to limitations to how concentrated the FXPs can be, and how much added salt is tolerated by the RRL. After incubation, each reaction was added to 180 μL of 1X binding buffer (25 mM HEPES pH 7.5, 75 mM NaCl, 0.5 mM EDTA, 0.1% Triton-X, 5% Glycerol, 4 mM $MgCl_2$) and incubated with 2.5 μL of equilibrated anti-FLAG M2 magnetic beads (Sigma-Aldrich) for at least 2 hours at 4°C. After the incubation, the solution was removed from the beads, and the beads were washed three times with 100

μL of 1X binding buffer. To elute the reporter peptide, 100 μL of FLAG peptide elution buffer (25 mM HEPES pH 7.5, 100 mM NaCl, 4 mM $MgCl_2$, 200 ng/μL 3X FLAG peptide (Sigma-Aldrich) was added to the beads. The elution was allowed to occur for at least 45 min at 4°C. The elution was subsequently removed, and the buffer evaporated (Savant Speed Vac Plus). Once all the liquid was removed, the remaining pellet was resuspended in 10 μL of H_2O.

To quantify the amount of reporter peptide by scintillation counting, 6 μL of the resuspended pellet solution was aliquoted onto 15 mm circular Whatman papers with a pore size of 11 μm (GE Healthcare LifeSciences), which were dried under a lamp for 10 minutes. The filter paper circles were transferred to scintillation vials and 4 mL of ScintiSafe 300% (Fisher Scientific) was added. The S-35 counts were recorded by reading for 1 min/sample using a scintillation counter (LS 6500, Beckman Coulter). If applicable, outliers (significance level set as 0.05) were removed. Results shown are from at least three trials where in each trial, percent activity values were calculated by normalizing to reactions without FXPs or protein added (n=3). For titrations and time trials, two trials were performed (n=2), except for the FMRP titration where four trials were performed for the 0 and 500 nM data points.

To visualize the production of reporter peptide, 3 μL of the resuspended pellet solution was aliquoted onto a piece of Whatman paper and dried under a lamp for 10 min. After drying, the paper placed in a phosphorimaging cassette, covered with Syran wrap, and placed under a phosphorimaging screen. After exposure, the phosphorimaging screen was scanned using a laser scanner (Typhoon FLA 9500, GE Healthcare) and the image was analyzed in ImageJ.

Time Course in vitro Translation Regulation of Renilla Luciferase mRNA by the Fragile X Proteins

The in vitro translation regulation of *Renilla* Luciferase mRNA by the FXPs and His_6-MBP was performed as described previously, with several modifications reported here [17]. Reaction buffer was added to contribute 4 mM HEPES KOH pH 7.8, 20 mM potassium acetate, and 0.6 mM $MgCl_2$ to the treated rabbit reticulocyte lysate (RRL). A 100 uL master reaction was made for each protein that contained 10nM of 5’ capped and 3’ poly A-tailed *Renilla* luciferase mRNA 500 nM FXP or His_6-MBP Samples were taken from this master reaction at 1, 30, 60, and 90 min during an incubation at 30 °C. At each time point, 18 μL of sample was combined with 2 μL of 30 μM colenterazine to achieve a final concentration of 3 μM colenterazine. The luminescence from reactions was analyzed using a multimode microplate reader (SPARK TECAN) as described previously.

Stability of NanoFX mRNAs in vitro

To test the stability of NanoFX mRNAs in the RRL system, reactions were set up as described previously with 2X RRL (treated with micrococcal nuclease to reduce endogenous mRNAs), water, 5′ capped NanoFX mRNAs with a 30-nucleotide 3′ poly (A) tail and fluorescein label, protein storage buffer or 500 nM of the corresponding protein. For these assays, RRL was supplemented with methionine instead of radioactive methionine. The reagents were combined in the order listed, mixed, and allowed to incubate for 75 min at 30°C. After reaction completion, the mRNA was purified using a Monarch RNA

Clean-up Kit (New England BioLabs) and the RNA was eluted using 1% sodium dodecyl sulfate warmed to 70°C. The purified mRNAs were then run on an 8% denaturing gel and visualized using a laser scanner (Typhoon FLA 9500, GE Healthcare). As a control, 1.5 pmol of each NanoFX mRNA was loaded. The gel image was analyzed, and the band intensities quantified in ImageJ.

Supplementary Material

Refer to Web version on PubMed Central for supplementary material.

Acknowledgements

We thank Youssi Athar for providing *Renilla* luciferase mRNA and the FMRP KH0-KH2 domains and the RGG motif. We thank Adam Maloney for providing 2X rabbit reticulocyte lysate, Reta Sarsam for providing His_6-MBP, and Justin Pi for confirming 5' capping of NanoFX mRNAs using eIF-4E. This work was supported by the National Institutes of Health (R01GM114261 and R35GM141864 to S.J.) and the Cell and Molecular Genetics Training Program funded by the National Institutes of Health (T32GM007240).

Data Availability

The data that support the findings of this study are available from the corresponding author on reasonable request.

References

[1]. Hagerman RJ, Berry-Kravis E, Hazlett HC, Bailey DB, Moine H, Kooy RF, Tassone F, Gantois I, Sonenberg N, Mandel JL, Hagerman PJ, Fragile X syndrome, Nat. Rev. Dis. Prim. 3 (2017) 17065. 10.1038/nrdp.2017.65. [PubMed: 28960184]

[2]. Darnell JC, Van Driesche SJ, Zhang C, Hung KYS, Mele A, Fraser CE, Stone EF, Chen C, Fak JJ, Chi SW, Licatalosi DD, Richter JD, Darnell RB, FMRP stalls ribosomal translocation on mRNAs linked to synaptic function and autism, Cell. 146 (2011) 247–261. 10.1016/j.cell.2011.06.013. [PubMed: 21784246]

[3]. Irwin SA, Patel B, Idupulapati M, Harris JB, Crisostomo RA, Larsen BP, Kooy F, Willems PJ, Cras P, Kozlowski PB, Swain RA, Weiler IJ, Greenough WT, Abnormal dendritic spine characteristics in the temporal and visual cortices of patients with fragile-X syndrome: A quantitative examination, Am. J. Med. Genet. 98 (2001) 161–167. 10.1002/1096-8628(20010115)98:2<161::AID-AJMG1025>3.0.CO;2-B. [PubMed: 11223852]

[4]. Chen E, Joseph S, Fragile X mental retardation protein: A paradigm for translational control by RNA-binding proteins, Biochimie. 114 (2015) 147–154. 10.1016/j.biochi.2015.02.005. [PubMed: 25701550]

[5]. Pieretti M, Zhang F, Fu Y-H, Warren ST, Oostra BA, Caskey CT, Nelson DL, Absence of expression of the FMR-1 gene in fragile X syndrome, Cell. 66 (1991) 817–822. 10.1016/0092-8674(91)90125-I. [PubMed: 1878973]

[6]. Sutcliffe JS, Nelson DL, Zhang F, Pieretti M, Caskey CT, Saxe D, Warren ST, DNA methylation represses *FMR-1* transcription in fragile X syndrome, Hum. Mol. Genet. 1 (1992) 397–400. 10.1093/hmg/1.6.397. [PubMed: 1301913]

[7]. Clifton NE, Rees E, Holmans PA, Pardiñas AF, Harwood JC, Di Florio A, Kirov G, Walters JTR, O'Donovan MC, Owen MJ, Hall J, Pocklington AJ, Genetic association of FMRP targets with psychiatric disorders, Mol. Psychiatry. (2020) 1–14. 10.1038/s41380-020-00912-2.

[8]. Siomi MC, Siomi H, Sauer WH, Srinivasan S, Nussbaum RL, Dreyfuss G, FXR1, an autosomal homolog of the fragile X mental retardation gene., Eur. Mol. Biol. Organ. J. (1995).

[9]. Zhang Y, O'Connor JP, Siomi MC, Srinivasan S, Dutra A, Nussbaum RL, Dreyfuss G, The fragile X mental retardation syndrome protein interacts with novel homologs FXR1 and FXR2., EMBO

J. 14 (1995) 5358. https://www.ncbi.nlm.nih.gov/pmc/articles/PMC394645/ (accessed May 21, 2020). [PubMed: 7489725]

[10]. Siomi MC, Zhang Y, Siomi H, Dreyfuss G, Specific sequences in the fragile X syndrome protein FMR1 and the FXR proteins mediate their binding to 60S ribosomal subunits and the interactions among them., Mol. Cell. Biol. 16 (1996) 3825–32. http://www.ncbi.nlm.nih.gov/pubmed/8668200 (accessed September 8, 2017). [PubMed: 8668200]

[11]. Bakker CE, de Diego Otero Y, Bontekoe C, Raghoe P, Luteijn T, Hoogeveen AT, Oostra BA, Willemsen R, Immunocytochemical and Biochemical Characterization of FMRP, FXR1P, and FXR2P in the Mouse, Exp. Cell Res. 258 (2000) 162–170. 10.1006/excr.2000.4932. [PubMed: 10912798]

[12]. Darnell JC, Fraser CE, Mostovetsky O, Darnell RB, Discrimination of common and unique RNA-binding activities among Fragile X mental retardation protein paralogs, Hum. Mol. Genet. 18 (2009) 3164–3177. 10.1093/hmg/ddp255. [PubMed: 19487368]

[13]. Guo W, Polich ED, Su J, Gao Y, Christopher DM, Allan AM, Wang M, Wang F, Wang G, Zhao X, Fragile X Proteins FMRP and FXR2P Control Synaptic GluA1 Expression and Neuronal Maturation via Distinct Mechanisms, Cell Rep. 11 (2015) 1651–1666. 10.1016/j.celrep.2015.05.013. [PubMed: 26051932]

[14]. Kirkpatrick LL, McIlwain KA, Nelson DL, Alternative Splicing in the Murine and Human FXR1 Genes, Genomics. 59 (1999) 193–202. 10.1006/GENO.1999.5868. [PubMed: 10409431]

[15]. Davidovic L, Sacconi S, Bechara EG, Delplace S, Allegra M, Desnuelle C, Bardoni B, Alteration of expression of muscle specific isoforms of the fragile X related protein 1 (FXR1P) in facioscapulohumeral muscular dystrophy patients., J. Med. Genet. 45 (2008) 679–85. 10.1136/jmg.2008.060541. [PubMed: 18628314]

[16]. Coy JF, Sedlacek Z, Bächner D, Hameister H, Joos S, Lichter P, Delius H, Poustka A, Highly conserved 3′ UTR and expression pattern of FXR1 points to a divergent gene regulation of FXR1 and FMR1, Hum. Mol. Genet. 4 (1995) 2209–2218. 10.1093/hmg/4.12.2209. [PubMed: 8634689]

[17]. Edwards M, Xu M, Joseph S, A simple procedure for bacterial expression and purification of the fragile X protein family, Sci. Rep. 10 (2020) 15858. 10.1038/s41598-020-72984-7. [PubMed: 32985615]

[18]. Myrick LK, Hashimoto H, Cheng X, Warren ST, Human FMRP contains an integral tandem Agenet (Tudor) and KH motif in the amino terminal domain, Hum. Mol. Genet. 24 (2015) 1733–1740. 10.1093/hmg/ddu586. [PubMed: 25416280]

[19]. Gantois I, Kooy RF, Targeting fragile X, Genome Biol. 3 (2002) reviews1014. http://www.ncbi.nlm.nih.gov/pubmed/12049671 (accessed October 3, 2017). [PubMed: 12049671]

[20]. Ramos A, Hollingworth D, Adinolfi S, Castets M, Kelly G, Frenkiel TA, Bardoni B, Pastore A, The Structure of the N-Terminal Domain of the Fragile X Mental Retardation Protein: A Platform for Protein-Protein Interaction, Structure. 14 (2006) 21–31. 10.1016/J.STR.2005.09.018. [PubMed: 16407062]

[21]. Adams-Cioaba MA, Guo Y, Bian C, Amaya MF, Lam R, Wasney GA, Vedadi M, Xu C, Min J, Structural Studies of the Tandem Tudor Domains of Fragile X Mental Retardation Related Proteins FXR1 and FXR2, PLoS One. 5 (2010) e13559. 10.1371/journal.pone.0013559. [PubMed: 21072162]

[22]. Järvelin AI, Noerenberg M, Davis I, Castello A, The new (dis)order in RNA regulation, (2016). 10.1186/s12964-016-0132-3.

[23]. Calabretta S, Richard S, Emerging Roles of Disordered Sequences in RNA-Binding Proteins, Trends Biochem. Sci. 40 (2015) 662–672. 10.1016/j.tibs.2015.08.012. [PubMed: 26481498]

[24]. Tamanini F, Kirkpatrick LL, Schonkeren J, van Unen L, Bontekoe C, Bakker C, Nelson D, Galjaard H, a Oostra B, a T. Hoogeveen, The fragile X-related proteins FXR1P and FXR2P contain a functional nucleolar-targeting signal equivalent to the HIV-1 regulatory proteins., Hum. Mol. Genet. (2000). 10.1093/hmg/9.10.1487.

[25]. Tan R, Frankel AD, A novel glutamine-RNA interaction identified by screening libraries in mammalian cells., Proc. Natl. Acad. Sci. U. S. A. 95 (1998) 4247–52. 10.1073/pnas.95.8.4247. [PubMed: 9539722]

[26]. Suhl JA, Chopra P, Anderson BR, Bassell GJ, Warren ST, Analysis of FMRP mRNA target datasets reveals highly associated mRNAs mediated by G-quadruplex structures formed via clustered WGGA sequences, Hum. Mol. Genet. 23 (2014) 5479–5491. 10.1093/hmg/ddu272. [PubMed: 24876161]

[27]. Ascano M, Mukherjee N, Bandaru P, Miller JB, Nusbaum JD, Corcoran DL, Langlois C, Munschauer M, Dewell S, Hafner M, Williams Z, Ohler U, Tuschl T, Tuschl T, FMRP targets distinct mRNA sequence elements to regulate protein expression., Nature. 492 (2012) 382–6. 10.1038/nature11737. [PubMed: 23235829]

[28]. Maurin T, Lebrigand K, Castagnola S, Paquet A, Jarjat M, Popa A, Grossi M, Rage F, Bardoni B, HITS-CLIP in various brain areas reveals new targets and new modalities of RNA binding by fragile X mental retardation protein., Nucleic Acids Res. 46 (2018) 6344–6355. 10.1093/nar/gky267. [PubMed: 29668986]

[29]. Whitman SA, Cover C, Yu L, Nelson DL, Zarnescu DC, Gregorio CC, Desmoplakin and talin2 are novel mRNA targets of fragile X-related protein-1 in cardiac muscle, Circ. Res. (2011). 10.1161/CIRCRESAHA.111.244244.

[30]. Davidovic L, Durand N, Khalfallah O, Tabet R, Barbry P, Mari B, Sacconi S, Moine H, Bardoni B, A Novel Role for the RNA-Binding Protein FXR1P in Myoblasts Cell-Cycle Progression by Modulating p21/Cdkn1a/Cip1/Waf1 mRNA Stability, PLoS Genet. (2013). 10.1371/journal.pgen.1003367.

[31]. Garnon J, Lachance C, Di Marco S, Hel Z, Marion D, Ruiz MC, Newkirk MM, Khandjian EW, Radzioch D, Fragile X-related protein FXR1P regulates proinflammatory cytokine tumor necrosis factor expression at the post-transcriptional level., J. Biol. Chem. 280 (2005) 5750–63. 10.1074/jbc.M401988200. [PubMed: 15548538]

[32]. Fernández E, Li KW, Rajan N, De Rubeis S, Fiers X, Smit AB, Achsel T, Bagni XC, Cellular/Molecular FXR2P Exerts a Positive Translational Control and Is Required for the Activity-Dependent Increase of PSD95 Expression, (n.d.). 10.1523/JNEUROSCI.4800-14.2015.

[33]. Xu X-L, Zong R, Li Z, Biswas MHU, Fang Z, Nelson DL, Gao F-B, FXR1P but not FMRP regulates the levels of mammalian brain-specific microRNA-9 and microRNA-124., J. Neurosci. 31 (2011) 13705–9. 10.1523/JNEUROSCI.2827-11.2011. [PubMed: 21957233]

[34]. Darnell JC, Fraser CE, Mostovetsky O, Stefani G, Jones TA, Eddy SR, Darnell RB, Kissing complex RNAs mediate interaction between the Fragile-X mental retardation protein KH2 domain and brain polyribosomes., Genes Dev. 19 (2005) 903–18. 10.1101/gad.1276805. [PubMed: 15805463]

[35]. Darnell JC, Jensen KB, Jin P, Brown V, Warren ST, Darnell RB, Fragile X mental retardation protein targets G quartet mRNAs important for neuronal function., Cell. 107 (2001) 489–99. 10.1016/s0092-8674(01)00566-9. [PubMed: 11719189]

[36]. Schaeffer C, Bardoni B, Mandel JL, Ehresmann B, Ehresmann C, Moine H, The fragile X mental retardation protein binds specifically to its mRNA via a purine quartet motif., EMBO J. 20 (2001) 4803–13. 10.1093/emboj/20.17.4803. [PubMed: 11532944]

[37]. Cook D, del Rayo Sanchez-Carbente M, Lachance C, Radzioch D, Tremblay S, Khandjian EW, DesGroseillers L, Murai KK, Fragile X Related Protein 1 Clusters with Ribosomes and Messenger RNAs at a Subset of Dendritic Spines in the Mouse Hippocampus, PLoS One. 6 (2011) e26120. 10.1371/journal.pone.0026120. [PubMed: 22022532]

[38]. Athar YM, Joseph S, RNA-Binding Specificity of the Human Fragile X Mental Retardation Protein, J. Mol. Biol. (2020). 10.1016/J.JMB.2020.04.021.

[39]. Lin C, Miles WO, Beyond CLIP: advances and opportunities to measure RBP–RNA and RNA–RNA interactions, Nucleic Acids Res. 47 (2019) 5490–5501. 10.1093/nar/gkz295. [PubMed: 31076772]

[40]. Vasilyev N, Polonskaia A, Darnell JC, Darnell RB, Patel DJ, Serganov A, Crystal structure reveals specific recognition of a G-quadruplex RNA by a β-turn in the RGG motif of FMRP, Proc. Natl. Acad. Sci. 112 (2015) E5391–E5400. 10.1073/pnas.1515737112. [PubMed: 26374839]

[41]. Goering R, Hudish LI, Guzman BB, Raj N, Bassell GJ, Russ HA, Dominguez D, Taliaferro JM, FMRP promotes RNA localization to neuronal projections through interactions between its RGG domain and G-quadruplex RNA sequences, Elife. 9 (2020). 10.7554/eLife.52621.

[42]. Wang E, Thombre R, Shah Y, Latanich R, Wang J, G-Quadruplexes as pathogenic drivers in neurodegenerative disorders, Nucleic Acids Res. 49 (2021) 4816–4830. 10.1093/nar/gkab164. [PubMed: 33784396]

[43]. Vasudevan S, Steitz JA, AU-Rich-Element-Mediated Upregulation of Translation by FXR1 and Argonaute 2, Cell. 128 (2007) 1105–1118. 10.1016/J.CELL.2007.01.038. [PubMed: 17382880]

[44]. Herman AB, Vrakas CN, Ray M, Kelemen SE, Sweredoski MJ, Moradian A, Haines DS, Autieri MV, FXR1 Is an IL-19-Responsive RNA-Binding Protein that Destabilizes Pro-inflammatory Transcripts in Vascular Smooth Muscle Cells, Cell Rep. (2018). 10.1016/j.celrep.2018.07.002.

[45]. Didiot M-C, Tian Z, Schaeffer C, Subramanian M, Mandel J-L, Moine H, The G-quartet containing FMRP binding site in FMR1 mRNA is a potent exonic splicing enhancer., Nucleic Acids Res. 36 (2008) 4902–12. 10.1093/nar/gkn472. [PubMed: 18653529]

[46]. Bechara E, Davidovic L, Melko M, Bensaid M, Tremblay S, Grosgeorge J, Khandjian EW, Lalli E, Bardoni B, Fragile X related protein 1 isoforms differentially modulate the affinity of fragile X mental retardation protein for G-quartet RNA structure, Nucleic Acids Res. 35 (2006) 299–306. 10.1093/nar/gkl1021. [PubMed: 17170008]

[47]. Kikin O, D'Antonio L, Bagga PS, QGRS Mapper: a web-based server for predicting G-quadruplexes in nucleotide sequences, Nucleic Acids Res. 34 (2006) W676–W682. 10.1093/nar/gkl253. [PubMed: 16845096]

[48]. Gruber AR, Lorenz R, Bernhart SH, Neubock R, Hofacker IL, The Vienna RNA Websuite, Nucleic Acids Res. 36 (2008) W70–W74. 10.1093/nar/gkn188. [PubMed: 18424795]

[49]. Athar YM, Joseph S, The Human Fragile X Mental Retardation Protein Inhibits the Elongation Step of Translation through Its RGG and C-Terminal Domains, Biochemistry. 59 (2020) 3813–3822. 10.1021/acs.biochem.0c00534. [PubMed: 32945655]

[50]. Karijolich J, Yu Y-T, Converting nonsense codons into sense codons by targeted pseudouridylation, Nature. 474 (2011) 395–398. 10.1038/nature10165. [PubMed: 21677757]

[51]. Fernández IS, Ng CL, Kelley AC, Wu G, Yu Y-T, Ramakrishnan V, Unusual base pairing during the decoding of a stop codon by the ribosome., Nature. 500 (2013) 107–10. 10.1038/nature12302. [PubMed: 23812587]

[52]. Davidovic L, Durand N, Khalfallah O, Tabet R, Barbry P, Mari B, Sacconi S, Moine H, Bardoni B, A Novel Role for the RNA–Binding Protein FXR1P in Myoblasts Cell-Cycle Progression by Modulating p21/Cdkn1a/Cip1/Waf1 mRNA Stability, PLoS Genet. 9 (2013) e1003367. 10.1371/journal.pgen.1003367. [PubMed: 23555284]

[53]. Adinolfi S, Ramos A, Martin SR, Dal Piaz F, Pucci P, Bardoni B, Mandel JL, Pastore A, The N-Terminus of the Fragile X Mental Retardation Protein Contains a Novel Domain Involved in Dimerization and RNA Binding †, Biochemistry. 42 (2003) 10437–10444. 10.1021/bi034909g. [PubMed: 12950170]

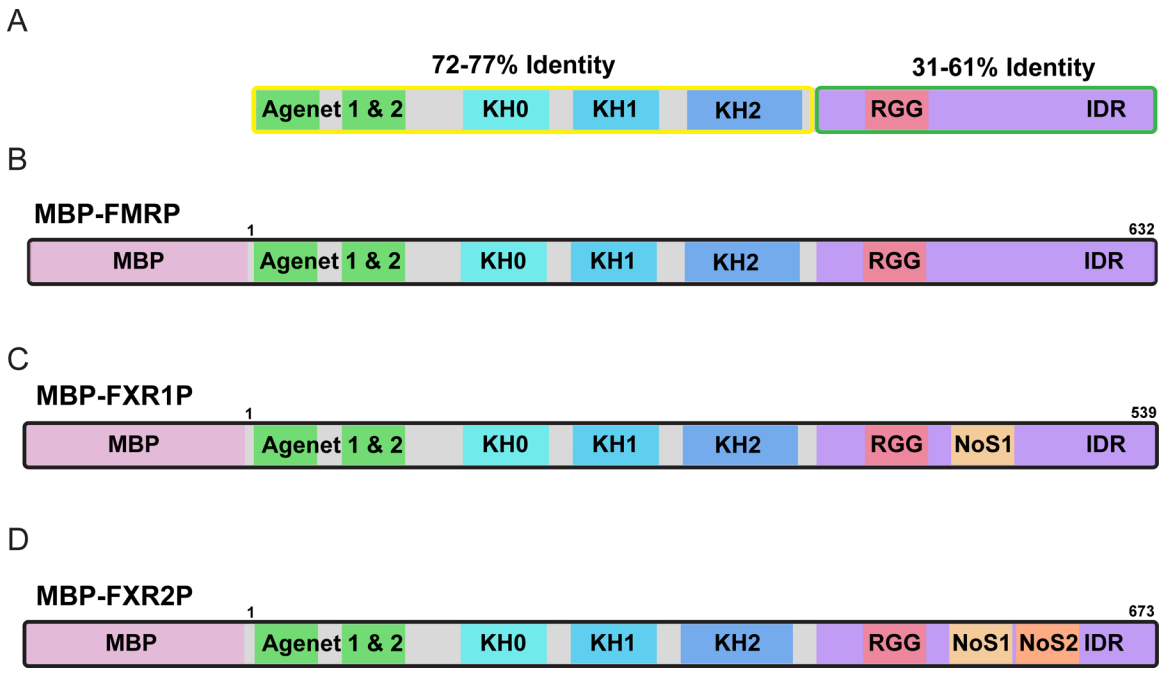

Figure 1.

Schematics of the fragile X proteins. (A) The fragile X proteins are multidomain proteins that are well-conserved through the sequence RQIG of each protein (outlined in yellow), but their conservation diverges after this point (outlined in green) [17]. (B-D) Schematics of protein constructs used in this article showing relevant domains. We used human FMRP isoform 1, human FXR1P isoform 2, and human FXR2P. Note all three FXP constructs are purified with an N-terminal maltose-binding protein tag (MBP).

A

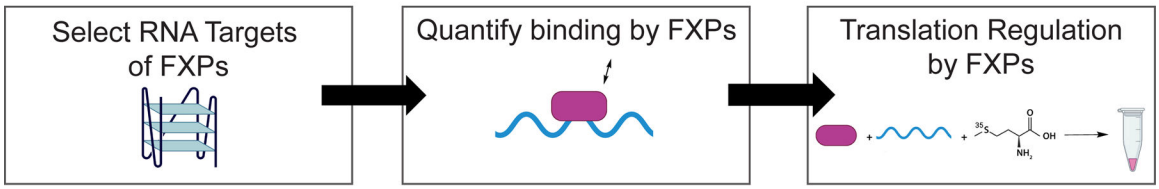

B

P21 γ: 5’-GGGGGUGUGUGGUGGUGGGGGUGGGCUUAUCUGGGAUGGGGU-3’

Mutant γ: 5’-GGGCCUCUCUCCUCCUCCCCCUCCCCUUAUCUCCCAUCCCCU-3’

N19: 5’-GGGGAAGAGGACAAGGAGGAAGAGGACGUGGAGGAGGCUUCU-3’

ARE: 5’-GGGAUUAUUUAUUAUUUAUUUAUUAUUUAUUUAUUUA-3’

C

Figure 2.

Systematic analysis of FXP RNA targets. (A) The workflow we used to characterize the FXPs’ interaction with, and influence on selected RNA targets. (B) Sequences selected for the three target RNAs and one negative control RNA (Mutant γ). (C) The NanoFX mRNAs consist of a 5’-methylguanosine cap, a Kozak sequence, a constant coding sequence which encodes a FLAG tag and four methionines, and a 30-nucleotide poly-A tail. For the reporters that contain a 3’ UTR, it is a constant 39-nucleotides but contains various target or control RNA sequences. Figure created with BioRender.

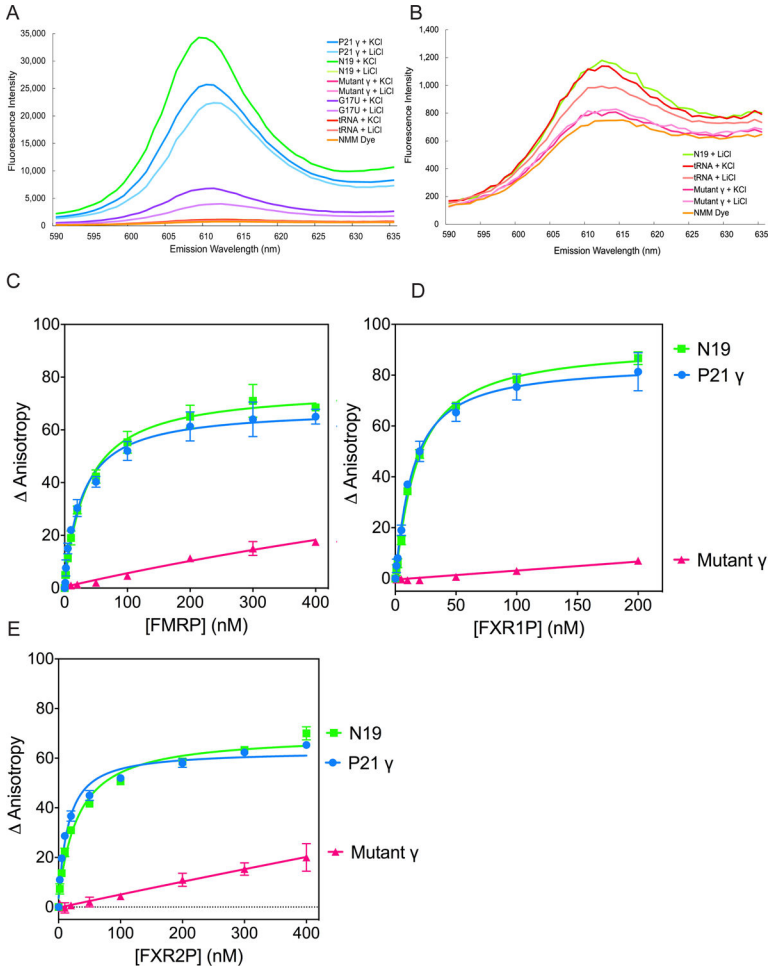

Figure 3.

The FXPs bind G-quadruplex-forming RNAs P21 γ and N19 with high affinity. (A) The NMM assay demonstrates that P21 γ and N19 (4 μM) form G-quadruplexes like the positive control RNA (G17U), indicated by the increase in fluorescence intensity after refolding in buffer with KCl. All other RNAs do not show fluorescence intensity after refolding in buffer with KCl, similar to the negative control (*E. coli* tRNA). One representative trial of two trials is shown. (B) Zoomed in on the graph Figure 3A to show the comparison between traces. FMRP (C), FXR1P (D), and FXR2P (E) bind P21 γ with high affinity (FMRP K_D = 27 ± 4 nM, FXR1P K_D = 12 ± 1 nM, and FXR2P K_D = 14 ± 2 nM) as well as N19 (FMRP K_D = 34 ± 4 nM, FXR1P K_D = 15 ± 1 nM, and FXR2P K_D = 29 ± 4 nM). All proteins show poor or no binding to Mutant γ (FMRP > 2 μM, FXR1P and FXR2P no binding). Results are from 3 or more independent trials with error bars displaying the standard deviation.

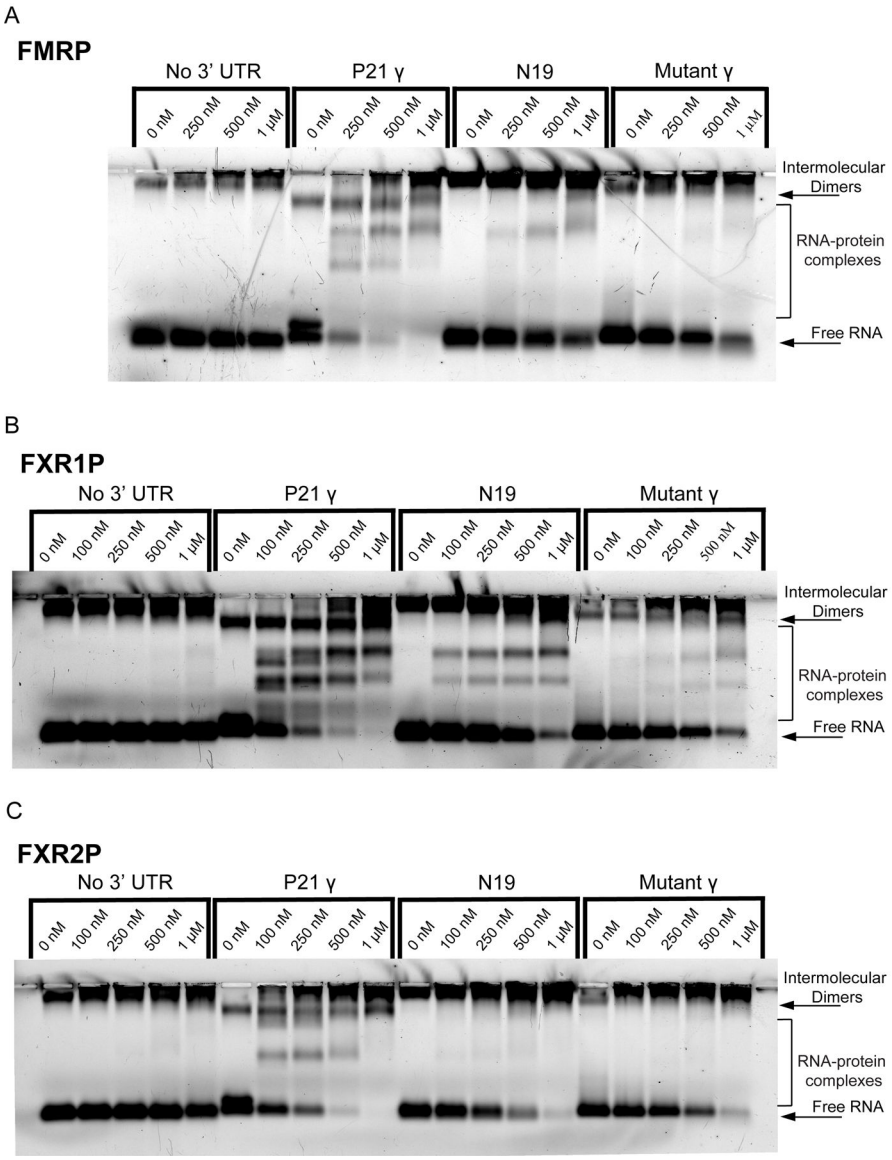

Figure 4.

The FXPs bind to NanoFX mRNAs with 3' UTR target sequences. (A-C) The FXPs show very little to no binding to the no 3' UTR NanoFX mRNA, stronger binding to the G-quadruplex NanoFX mRNAs (P21 γ & N19), and weak to moderate binding to Mutant γ NanoFX mRNA. The concentration of each FXP was increased from 0 to 1 μM, as indicated above the lanes.

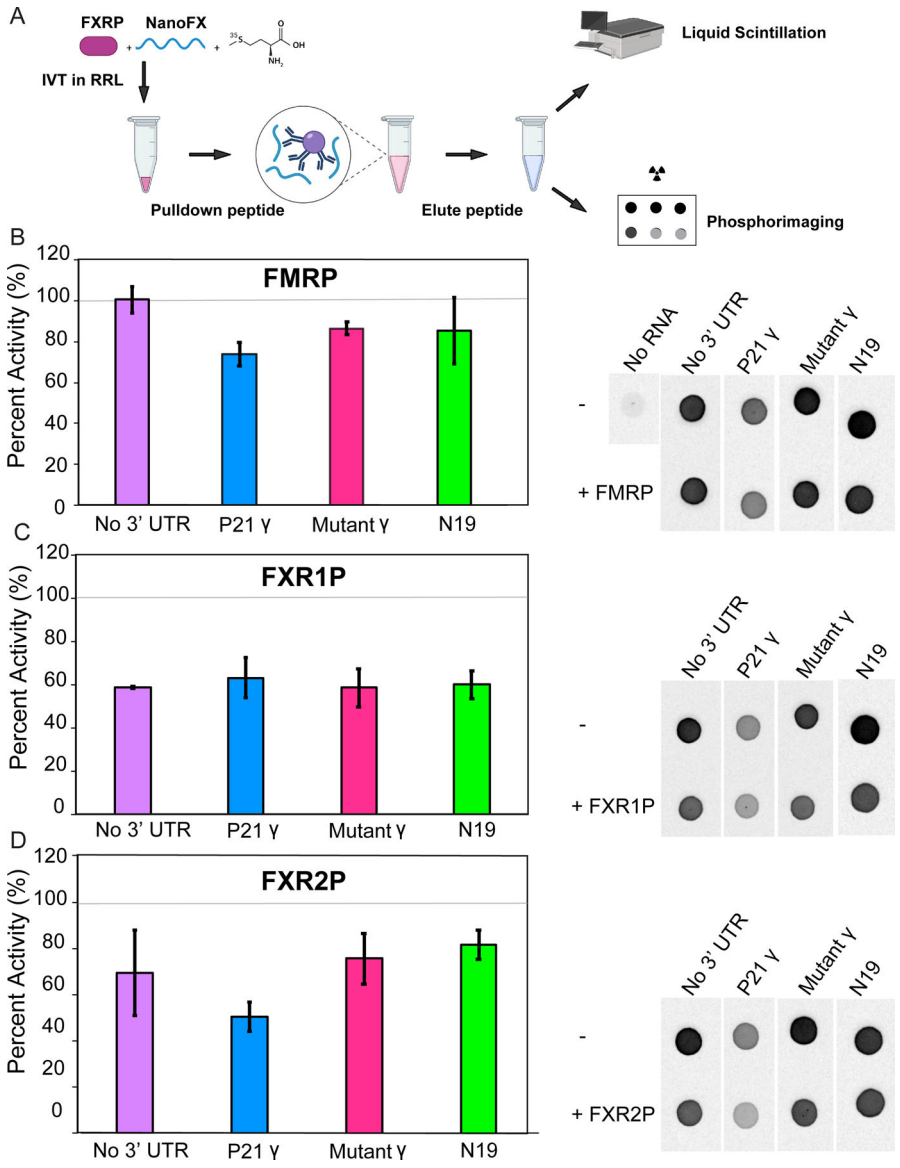

Figure 5.

In vitro translation assay workflow and results for FXPs. (A) To validate the FXPs' influence on target RNAs, we tested the FXPs' ability to alter their translatability in rabbit reticulocyte lysate (RRL) lacking methionine (-MET). Radioactive MET is incorporated into our reporter peptide, which we purified from other proteins in the system using a FLAG affinity purification. We quantified the abundance of our reporter peptide through liquid scintillation counting. The results were subsequently visualized through phosphorimaging. Figure created with BioRender. (B) FMRP does not affect the translation of the no 3' UTR NanoFX mRNA but inhibits all NanoFX mRNAs with 3' UTRs (no 3' UTR 100 ± 6%, P21 γ 74 ± 6%, Mutant γ 86 ± 3%, and N19 85 ± 16%). Results are from three independent trials where, in each trial, values were normalized to reactions with FXP protein storage buffer added instead of FXPs (n =3). Error bars display the standard deviation. (C) FXR1P inhibits all NanoFX mRNAs to a similar extent (no 3' UTR 59 ± 1%, P21 γ 63

± 9%, Mutant γ 59 ± 9%, and N19 60 ± 7%). Results are from at least three independent trials where in each trial, values were normalized to reactions with FXP protein storage buffer added instead of FXPs. Error bars display the standard deviation. (D) FXR2P has an inhibitory effect on all NanoFX mRNAs, but inhibition of the P21 γ NanoFX mRNA is the greatest (no 3' UTR 69 ± 18%, P21 γ 51 ± 6%, Mutant γ 76 ± 11%, and N19 82 ± 6%). Results are from four independent trials, with one outlier value for P21 γ NanoFX mRNA removed (n=4). For all FXPs, phosphorimaging results were taken in all trials, with a representative image shown.

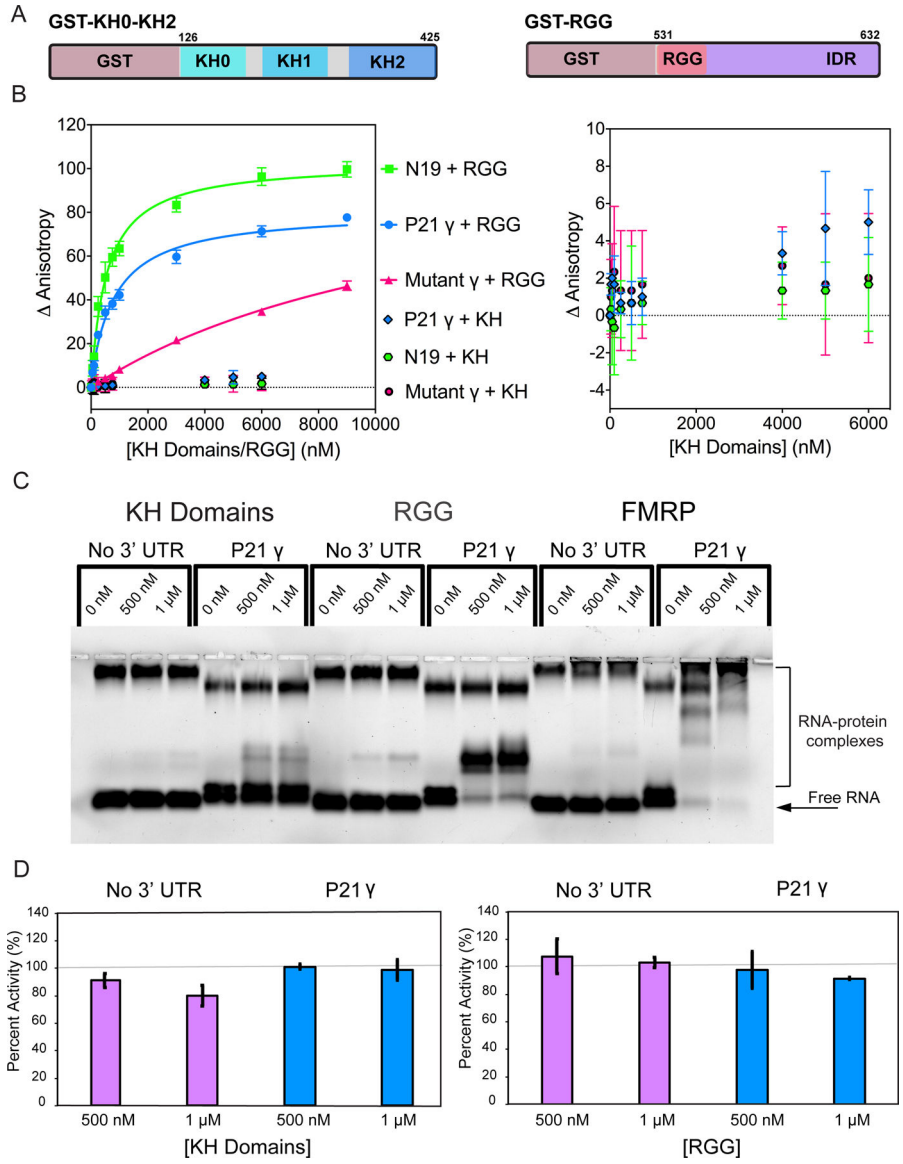

Figure 6.

RNA-binding and IVT studies with FMRP's KH domains and RGG motif. (A) Schematic of the two glutathione S-transferase-tagged FMRP constructs used to compare the functions of FMRP's two classes of RNA-binding domains. (B) The RGG motif principally binds to the G-quadruplex RNAs (N19 K_D = 550 ± 50 nM, P21 γ K_D = 830 ± 70 nM, Mutant γ K_D = 13 ± 2 μM), while the KH domains did not bind any of the RNAs tested. The graph on the right shows the zoomed in view of the binding data for the construct with the KH domains. Error bars display the standard deviation of three or more independent trials. (C) The KH domains do not bind the target RNA sequences within the context of the NanoFX mRNAs. Similar to full-length FMRP, the RGG motif binds the P21 γ NanoFX mRNA, but not the no 3' UTR NanoFX mRNA. The concentration of each FXP were increased from 0 to 1 μM, as indicated above the lanes. (D) The KH domains only slightly inhibited the no 3' UTR NanoFX mRNA (91 ± 5% at 500 nM and 80 ± 8% at 1 μM) but did not significantly

alter translation of the P21 γ NanoFX mRNA (101 ± 2.0% at 500 nM and 99 ± 7% at 1 μM). Similar to full-length FMRP, the RGG motif did not inhibit the no 3' UTR NanoFX mRNA (108 ± 13% at 500 nM and 103 ± 4% at 1 μM). The RGG motif slightly inhibited P21 γ NanoFX mRNA, but only at 1 μM (98 ± 13% at 500 nM and 92 ± 1% at 1 μM). Results are from three independent trials (n=3) where in each trial, values were normalized to reactions with protein storage buffer added instead of protein. Error bars display the standard deviation.

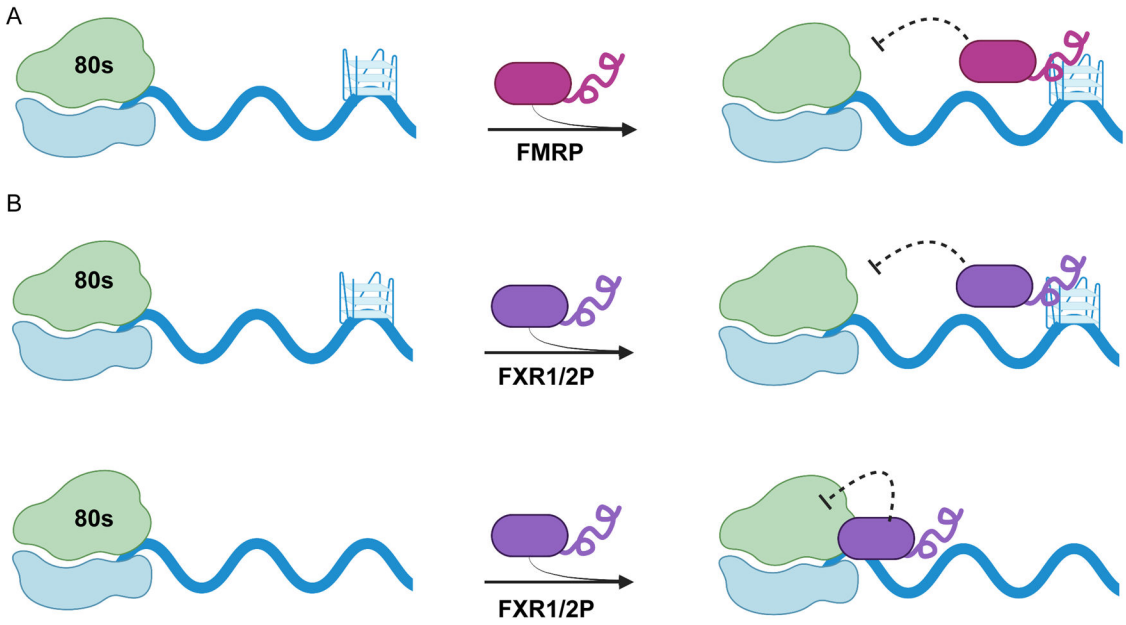

Figure 7.

The fragile X proteins differentially regulate translation of mRNAs. (A). FMRP's inhibition of translation correlates with its binding to mRNA. FMRP was found to bind with the highest affinity to mRNAs with G-quadruplex structures, and this binding occurs primarily due to the RGG motif/C-terminal domain. Therefore, FMRP may bind to G-quadruplexes within mRNAs to inhibit translation. (B). FXR1P/2P likewise bind with the highest affinity to mRNAs with G-quadruplex structures. However, their inhibition of translation does not correlate with their binding to mRNA. Rather, FXR1/2P appear to globally inhibit translation. We propose that FXR1/2P may be able to bind target mRNA structures to inhibit translation and/or bind to the ribosome to globally inhibit translation.